Synthesis and characterization of non-stoichiometric nickel-copper manganites

Christophe Drouet, Pierre Alphonse, Abel Rousset

Synthesis and characterization of non-stoichiometric nickel–copper manganites

Christophe Drouet*, Pierre Alphonse, Abel Rousset

Laboratoire de Chimie des Matériaux Inorganiques et Energétiques, 118 Route de Narbonne, 31062 Toulouse Cedex, France

Abstract

Non-stoichiometric nickel–copper manganites $Ni_xCu_yMn_{3-x-y}\square_{3\delta/4}O_{4+\delta}$ were synthesized by thermal decomposition of mixed $Ni_{x/3}Cu_{y/3}Mn_{(3-x-y)/3}C_2O_4$, nH_2O oxalates in air at low temperature (623–673 K). X-ray diffraction showed that, for a nickel content $x_{Ni} \geq 0.1$, the oxalates precipitated presented a mixed crystal structure up to a limit value of copper extent, whereas the oxalates obtained with $x_{Ni} < 0.1$ were not mixed. This could be explained by the intermediate structure of nickel oxalate (β orthorhombic form) between those of copper and manganese (α monoclinic form) oxalates. The structure (α or β) of the mixed oxalates obtained was also investigated and their lattice parameters are given. The $Ni_xCu_yMn_{3-x-y}\square_{3\delta/4}O_{4+\delta}$ oxides crystallize in the spinel structure in a wide range of composition and a stabilizing effect of copper was evidenced. They are highly divided ($Sw > 100\ m^2\ g^{-1}$) however Sw tends to decrease with increasing y_{Cu}. The non-stoichiometry δ of such nickel–copper manganites was for the first time determined by selective titration (gas chromatography) of the oxygen released during TPR experiments in argon. The technique is presented and the results, along with those obtained with manganese oxide Mn_5O_8 and nickel manganites synthesized in the same conditions, showed that δ depended both on the decomposition temperature of the oxalate and on the chemical composition of the oxide. Such results should provide interesting data concerning the cationic distributions of these non-stoichiometric nickel–copper manganites.

Keywords: Spinel; Nickel–copper manganite; Mixed oxalate; Non-stoichiometry

1. Introduction

Stoichiometric nickel–copper manganites have already been studied as negative temperature coefficient (NTC) thermistors since they possess interesting electrical properties such as low resistivity and electrical stability [1,2]. These oxides are generally prepared by thermal decomposition of mixed nickel–copper–manganese oxalates in air at high temperature (1173 K) and have low specific surface areas (close to $1\ m^2\ g^{-1}$). Non-stoichiometric manganites synthesized at low temperature (623 K) have recently attracted much interest. Such oxides are cation-deficient and highly divided with large specific surface areas ($> 100\ m^2\ g^{-1}$), which may be an advantage in order to prepare high density ceramics

*Corresponding author. Tel.: +33-5-6155-6285; fax: +33-5-6155-6163.

E-mail address: alphonse@iris.ups-tlse.fr (C. Drouet)

at reduced sintering temperatures [3,4]. Moreover, non-stoichiometric nickel manganites $Ni_xMn_{3-x}\square_{3\delta/4}O_{4+\delta}$ were found to be very reactive towards CO total oxidation [5]. However, these nickel manganites are relatively unstable when heated in air.

The aim of this paper is to report structural features of non-stoichiometric Ni–Cu–Mn spinels and their oxalate precursors. The main results were obtained by thermal analyses (TGA, DTA, Temperature-Programmed-Reduction) and X-ray diffraction. The effects of the introduction of copper in the structure on the thermal stability, surface area and non-stoichiometry of the oxides are discussed.

2. Experimental

2.1. Preparation of samples

Non-stoichiometric $Ni_xMn_{3-x}\square_{3\delta/4}O_{4+\delta}$ and $Ni_xCu_yMn_{3-x-y}\square_{3\delta/4}O_{4+\delta}$ manganites were synthesized by thermal decomposition of mixed oxalates $Ni_{x/3}Mn_{(3-x)/3}C_2O_4$, nH_2O and $Ni_{x/3}Cu_{y/3}Mn_{(3-x-y)/3}C_2O_4$, nH_2O respectively, at low temperature (623–673 K) in air for 6 h at a heating rate of 2 K min^{-1}. These oxalate precursors were precipitated at room temperature by the quick introduction of an aqueous solution of nickel and manganese nitrates or nickel, copper and manganese nitrates, respectively (0.2 M) into an aqueous solution of ammonium oxalate 0.2 M at room temperature under stirring. After 30 min, the precipitate was filtered, washed with deionized water and dried at 360 K in air.

Non-stoichiometric manganese oxide $Mn_5O_{8+\delta}$ was obtained by thermal decomposition of manganese oxalate MnC_2O_4, $2H_2O$ at 623 K in air for 6 h.

2.2. Characterization of samples

The determination of the crystallographic structure of the samples was performed by X-ray diffraction with a Siemens D501 diffractometer using either $CoK\bar{\alpha}$ ($\lambda_{Co} = 0.17902$ nm) or the $CuK\bar{\alpha}$ radiation ($\lambda_{Cu} = 0.15418$ nm).

The chemical compositions were determined by ionic chromatography (Dionex DX100, cationic column CS5).

The measurement of the specific surface area of the oxides was performed by nitrogen adsorption at 77 K on a Micromeritics Flowsorb II 2300 apparatus using the Brunauer-Emmett-Teller (BET) method.

Thermogravimetric (TGA) and differential thermal analyses (DTA) were carried out on a Setaram TG-DTA 92 microbalance with 20 mg of sample and alumina as a reference. The experiments were performed in air at a heating rate of 2.5 K min^{-1} from room temperature to 973 K.

The non-stoichiometry δ of the oxides was determined through Temperature Programmed Reduction followed both by thermogravimetric and gas chromatography analyses. The experiments were carried out in a vertical plug flow reactor. The mass variation of the oxide (initially 60 mg) was followed with a Cahn D200 electrobalance. The sample was first degassed (1 Pa) at room temperature for 1 h and the reactor was filled with Ar, maintaining a flow of 15 cm^3 min^{-1}. The temperature was then increased linearly with a heating rate of 5 K min^{-1} up to 900 K. Every 120 s, the gas flowing out of the reactor was sampled and analyzed by gas chromatography (Shimadzu GC-8A, detector: TCD, carrier gas: argon, column: molecular sieve 13 ×). These analyses allow us to follow the amount of oxygen released upon heating the oxides in argon and hence enable us to evaluate δ.

This technique presents the advantage to quantify selectively the non-stoichiometric oxygen, without preliminary dissolution as in chemical titration methods.

Moreover, the accuracy of the results obtained was periodically checked by heating a known mass of Mn_2O_3, which gives a known quantity of oxygen during its reduction to Mn_3O_4 (the reduction of CuO to Cu_2O was also used).

Of course, this method can only be used if the heating of non-stoichiometric oxides give stoichiometric oxides.

3. Results and discussion

3.1. Structure and characterization of the oxalates

In order to synthesize mixed oxides at low tem-

perature, mixed oxalate precursors must be used [6]. Both manganese and nickel oxalates belong to the magnesium series (Mg, Mn, Fe, Co, Ni, Zn). In the experimental conditions used here, the manganese oxalate crystallizes in the α form (humboldtine-type, space group C2/c, monoclinic but which can also be described by a pseudo-orthorhombic cell [7,8]) and the nickel oxalate in the β form (space group Cccm, orthorhombic [9]). Both α and β are composed of piled-up leaves, each leaf being constituted by parallel oxalate ribbons, and the cohesion of the structure results from hydrogen bonds between the ribbons thanks to H_2O molecules [7]. The oxalates belonging to the magnesium series contain generally two structural water molecules as in MnC_2O_4, $2H_2O$ or NiC_2O_4, $2H_2O$, for example. Whereas αMnC_2O_4, $2H_2O$ may be perfectly described by the humboldtine structure, βNiC_2O_4, $2H_2O$ present stacking faults when compared to this structure. Indeed in this last case some of the leaves play the role of twin planes [7–10]. In this way, these allotropic forms differ from each other by the presence or the absence of these twin planes in their structure.

Copper oxalate does not belong to the magnesium series and has a different crystalline structure. In this case, the oxalate ribbons are located on leaves which are not parallel but involved in a three-dimensional arrangement in which they are perpendicular to one another, which maintains the cohesion of the structure [11]. Water does not play any role in the cohesion of the copper oxalate structure, and different water contents are proposed in the literature (CuC_2O_4, $1/3H_2O$, CuC_2O_4, $0.4H_2O$, CuC_2O_4,$1/2H_2O$) [11–13]. Fichtner-Schmittler [11] has determined the monoclinic structure (space group $P2_1/c$) of copper oxalate in the case of *ordered* crystals, but the most common *disordered* crystals of copper oxalate (containing stacking faults) may be described by an orthorhombic cell.

X-ray diffraction showed the impossibility to obtain mixed copper–manganese oxalates without a minimum amount of nickel $x_{Ni} \geq 0.1$ (where x_{Ni} stands for the nickel content of the final spinel oxide). However, beyond a maximum limit of copper content (which depends on x_{Ni} and that we have evaluated to ca. 0.8 for $x_{Ni} = 0.1$ and 0.9 for $x_{Ni} = 0.2$) XRD analyses showed the presence of copper oxalate beside a mixed Ni–Cu–Mn oxalate. Between these limits, the oxalates precipitated presented a mixed crystal structure.

Consequently, the introduction of nickel allowed us to prepare mixed oxalates containing at the same time copper and manganese. Nickel oxalate (whose orthorhombic crystalline structure presents numerous stacking faults) may have an intermediate form between those of copper oxalate (pseudo-orthorhombic) and manganese oxalate (monoclinic), allowing the copper to fit to the manganese oxalate structure. This interpretation recalls that proposed by Villette [14] in the case of mixed copper–iron oxalates, who found that in hydro-alcoholic solutions (which favour the β form of the oxalates of the magnesium series) the precipitation of mixed Fe-Cu oxalates occurred whereas it was impossible in aqueous solution (where the α form predominates).

The lattice parameters of some nickel–copper–manganese mixed oxalates prepared have been reported in Table 1. These oxalates crystallize either in the α monoclinic form or in the β orthorhombic form (see typical XRD diagrams in Fig. 1) depending on their nickel and copper contents. Indeed, for a given copper content y_{Cu} the increase of x_{Ni} leads to the

Table 1
Experimental lattice parameters of some mixed Ni–Cu–Mn oxalates $Ni_{x/3}Cu_{y/3}Mn_{(3-x-y)/3}C_2O_4$, nH_2O

Composition			Lattice parameters of $Ni_{x/3}Cu_{y/3}Mn_{(3-x-y)/3}C_2O_4$, nH_2O				Allotropic form
x_{Ni}	y_{Cu}	Mn	$a \pm 0.05$ Å	$b \pm 0.05$ Å	$c \pm 0.05$ Å	$\beta \pm 0.50°$	α or β
0.14	0.30	2.56	12.01	5.63	9.98	128.1	α
0.22	0.30	2.48	11.92	5.61	9.87	128.2	α
0.26	0.30	2.44	11.99	5.60	9.99	128.7	α
0.70	0.30	2.00	12.11	5.32	15.35	–	β
0.70	0.65	1.65	11.92	5.47	15.64	–	β
0.70	0.75	1.55	11.86	5.44	15.71	–	β
0.70	0.91	1.39	11.87	5.42	15.71	–	β

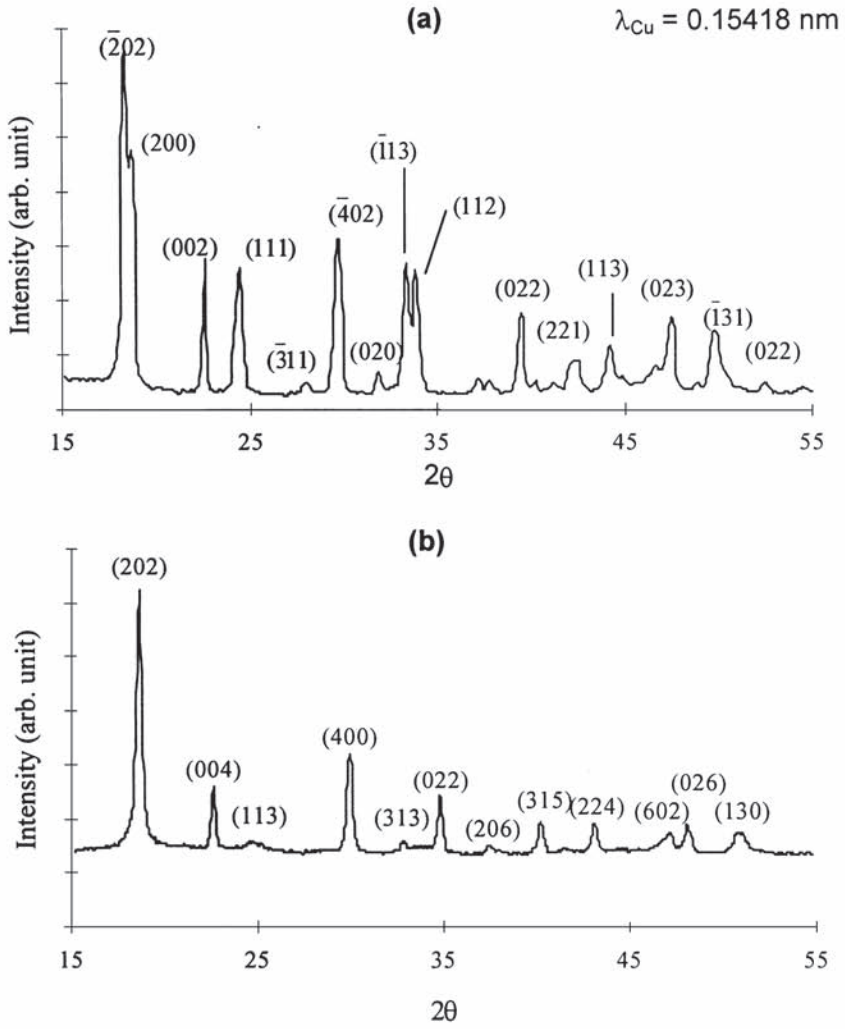

Oxalate	Experimental lattice parameters			
	a ± 0.05 Å	b ± 0.05 Å	c ± 0.05 Å	β°
$Ni_{0.26/3}Cu_{0.30/3}Mn_{2.44/3}C_2O_4$, nH_2O (α)	11.99	5.60	9.99	128.70
$Ni_{0.70/3}Cu_{0.75/3}Mn_{1.55/3}C_2O_4$, nH_2O (β)	11.86	5.44	15.71	_

Fig. 1. Experimental XRD pattern of (a) oxalate $Ni_{0.26/3}Cu_{0.30/3}Mn_{2.44/3}C_2O_4$, nH_2O (α form), (b) oxalate $Ni_{0.70/3}Cu_{0.75/3}Mn_{1.55/3}C_2O_4$, nH_2O (β form).

evolution from α to β, which is evidenced by the progressive disappearance of some peaks in the XRD diagrams (Fig. 2). Moreover, it is worthwhile to note that when the manganese content becomes too low (at least if the nickel content is sufficient) the corresponding oxalate crystallizes in the β form.

However, one has to keep in mind that the preparation route used to synthesize such oxalates (pH, temperature, stirring conditions, solvent, etc.) determines the allotropic forms obtained. Indeed, Töpfer et al. [15] found that nickel and nickel–manganese oxalates, precipitated by adding oxalic acid to a solution of nickel and manganese carbonates in acetic acid, crystallized all in the α monoclinic form.

Thermogravimetric analyses show that the thermal

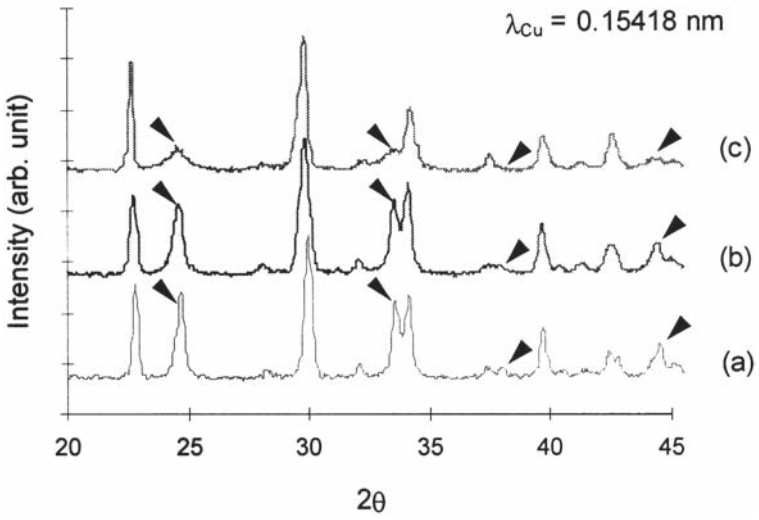

Fig. 2. Evolution of the XRD diagrams from the α to the β form for $Ni_{x/3}Cu_{y/3}Mn_{(3-x-y)/3}C_2O_4$, nH_2O with $y_{Cu}=0.3$, and (a) $x_{Ni}=0.2$ (α form), (b) $x_{Ni}=0.3$ (α form), (c) $x_{Ni}=0.7$ (β form).

decomposition in air of the mixed oxalates occurs in two steps as can be seen in Fig. 3(a) in the case of $Ni_{0.70/3}Cu_{0.65/3}Mn_{1.65/3}C_2O_4$, nH_2O. The first one (endothermic) is relative to the dehydration of the oxalate and the second (overall exothermic) is actually relative to the superimposition of two mechanisms: the decomposition of the oxalate functional group (endothermic) with loss of CO_2 (mass spectrometry shows the absence of CO in the gas phase, the carbon monoxide formed during the decomposition is completely oxidized into carbon dioxide) and the quick oxidation of the products (exothermic) [16], which can be generally written as follows:

$$Ni_{x/3}Cu_{y/3}Mn_{(3-x-y)/3}C_2O_4, nH_2O \rightarrow$$
$$Ni_{x/3}Cu_{y/3}Mn_{(3-x-y)/3}C_2O_4 + nH_2O$$

$$Ni_{x/3}Cu_{y/3}Mn_{(3-x-y)/3}C_2O_4 + 2/3O_2 \rightarrow$$
$$1/3Ni_xCu_yMn_{3-x-y}O_4 + 2CO_2$$

If the same analysis is carried out on a mixture of Ni–Mn mixed oxalate and Cu oxalate in mass proportions corresponding to those of $Ni_{0.70/3}Cu_{0.65/3}Mn_{1.65/3}C_2O_4$, nH_2O (7.5% Ni, 7.6% Cu), the DTA profile obtained shows then two distinguishable exothermic peaks corresponding to the decomposition of Cu oxalate and Ni–Mn oxalate, respectively [Fig. 3(b)]. Thus, DTA analyses enable us to distinguish a mixed oxalate from a mixture of oxalates, confirming the XRD results.

The dehydration and decomposition temperatures of the oxalates (determined by TGA and DTA) vary with their chemical composition, as shown in Table 2. These experiments show that the dehydration temperature slightly decreases when y_{Cu} increases. Such a variation can be explained by the fact that copper oxalate contains less structural water than nickel and manganese oxalates. On the other hand, the decomposition temperature of the oxalates increases with increasing y_{Cu}, which in turn shows a stabilizing effect of copper for the oxalate structure.

3.2. Structure and characterization of the oxides

X-ray diffraction shows that alike nickel manganites, nickel–copper manganites crystallize in the spinel structure. However, as was said before, the synthesis of mixed $Ni_xCu_yMn_{3-x-y}O_4$ oxides at low temperature can only be performed from mixed oxalates. Indeed, the decomposition of the oxalate corresponding to $x_{Ni}=0.70$ and $y_{Cu}=1.10$ (which is actually a mixture of a mixed Ni–Cu–Mn oxalate and Cu oxalate) does not lead to a mixed oxide but to CuO beside the spinel phase (Fig. 4).

In order to study the thermal stability of nickel–copper manganites, X-ray diffraction experiments

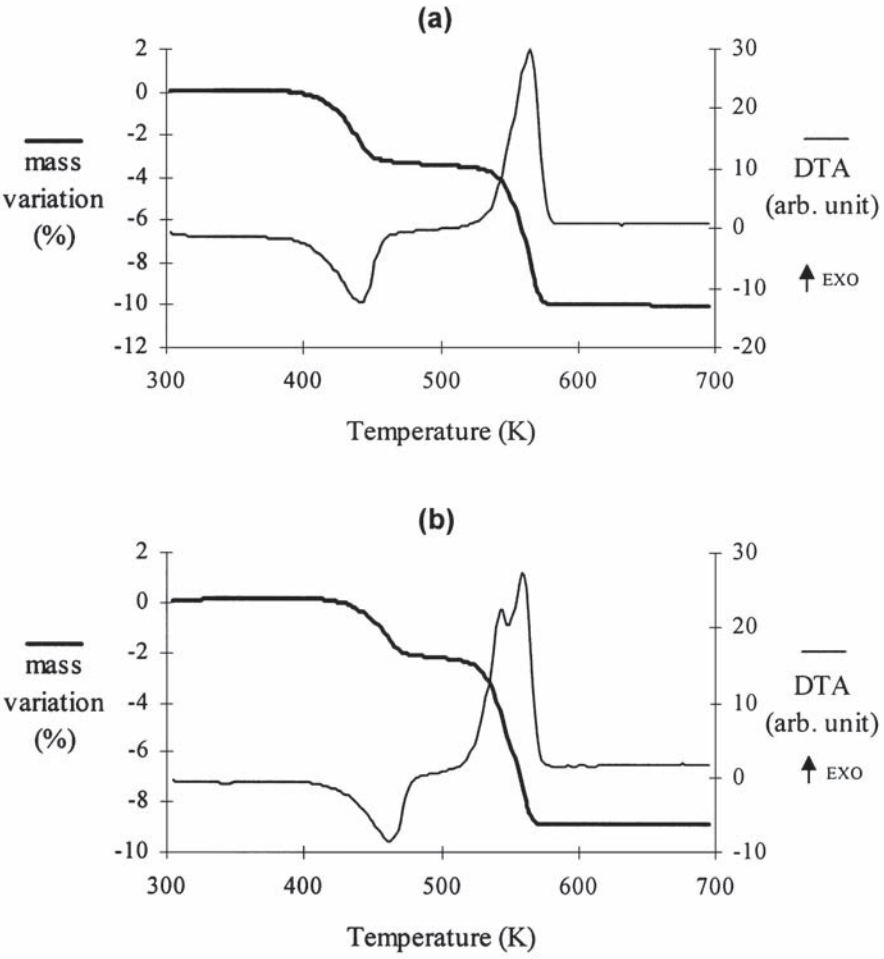

Fig. 3. TGA and DTA profiles for the thermal decomposition of (a) $Ni_{0.70/3}Cu_{0.65/3}Mn_{1.65/3}C_2O_4$, nH_2O (heating rate 2.5 K min^{-1}, $m=20$ mg), (b) a mixture of a Ni–Mn mixed oxalate and Cu oxalate with 7.5% Ni and 7.6% Cu (heating rate 2.5 K min^{-1}, total mass = 20 mg).

Table 2
Evolution of the dehydration and decomposition temperatures with y_{Cu} for $Ni_{0.70/3}Cu_{y/3}Mn_{(2.30-y)/3}C_2O_4$, nH_2O

y_{Cu}	T dehydration (K)	T decomposition (K)
0	465	535
0.26	453	540
0.65	439	560
0.91	423	565

were performed on $Ni_{0.70}Cu_{0.65}Mn_{1.65}O_4$ synthesized by thermal decomposition in air of $Ni_{0.70/3}Cu_{0.65/3}Mn_{1.65/3}C_2O_4$, nH_2O at different temperatures ranging from 673 to 973 K (Fig. 5(a)). Similar XRD experiments were also performed on nickel manganite $Ni_{0.70}Mn_{2.30}O_4$ [Fig. 5(b)]. These results show that $Ni_{0.70}Cu_{0.65}Mn_{1.65}O_4$ keeps the spinel structure in the whole range of decomposition temperature studied (623-973 K), whereas $Ni_{0.70}Mn_{2.30}O_4$ decomposes into a mixture of $NiMnO_3$ and αMn_2O_3 between ca. 773 K and 980 K [Fig. 5(b)] which is consistent with the phase diagram proposed by Wickham [17].

The absence of such a decomposition in the case of $Ni_{0.70}Cu_{0.65}Mn_{1.65}O_4$ shows clearly that copper exhibits a stabilizing effect for the spinel structure. However, Töpfer et al. [18] found that the spinels of the system $Cu_xNiMn_{2-x}O_4$ were actually metastable phases leading to partial decomposition upon long-term annealing. The same conclusion can be drawn concerning the oxides presented in this paper since a thermal treatment at 773 K for 100 h leads to the appearance of an ilmenite-like phase beside the spinel (Fig. 6).

The specific surface areas Sw of the mixed nickel–

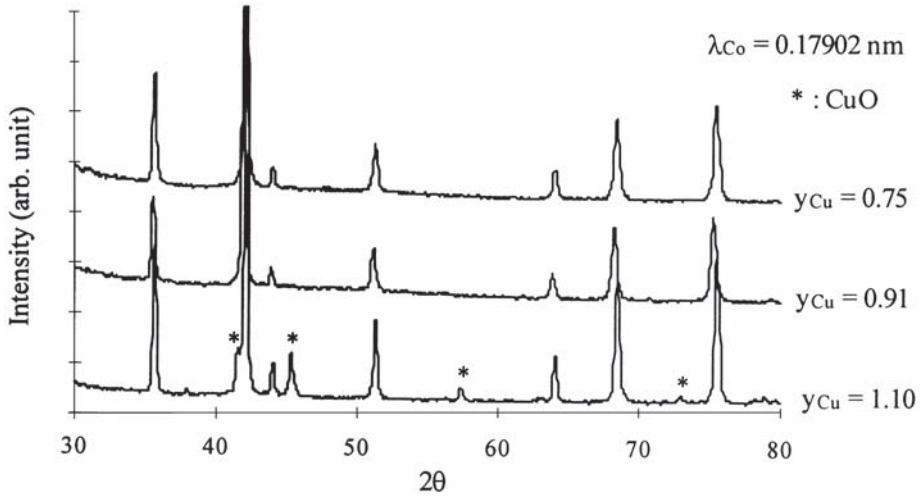

Fig. 4. XRD patterns for $Ni_{0.70}Cu_yMn_{2.30-y}O_4$ synthesized at 973 K with $y_{Cu}=0.65$, 0.91 and 1.10.

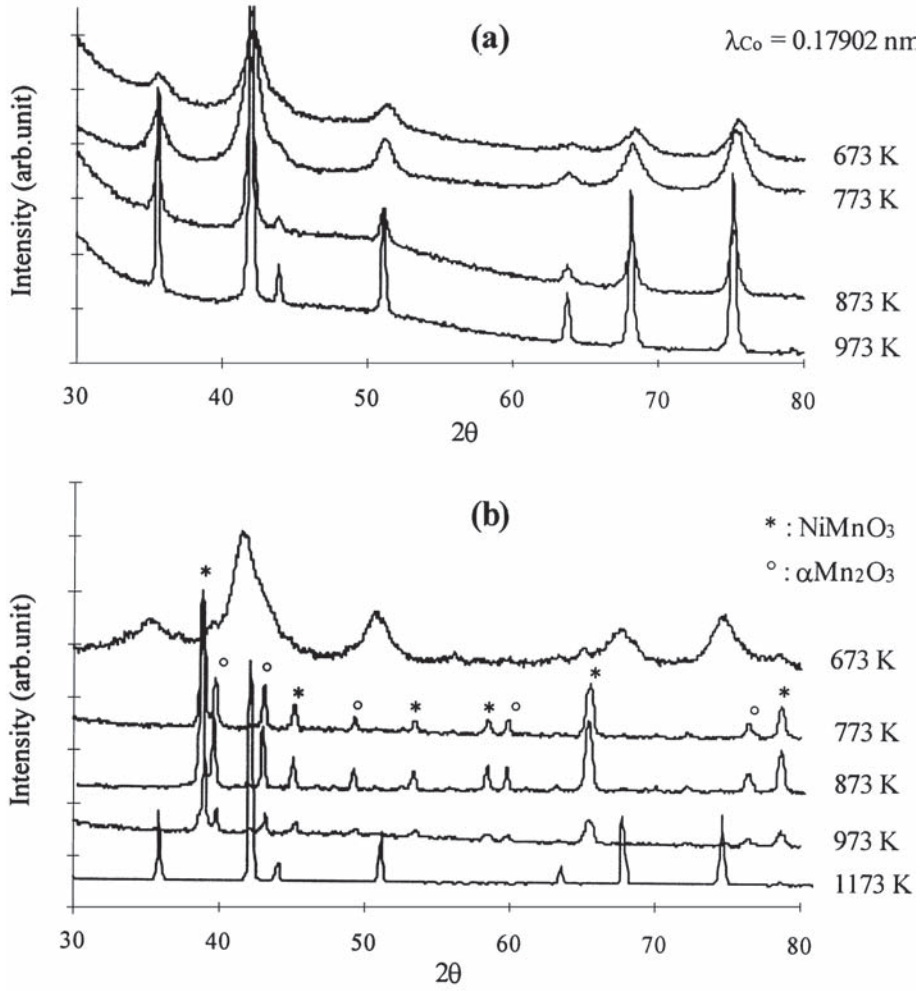

Fig. 5. XRD patterns for (a) nickel–copper manganite $x_{Ni}=0.70$, $y_{Cu}=0.65$, and (b) nickel manganite $x_{Ni}=0.70$ synthesized in air at different temperatures.

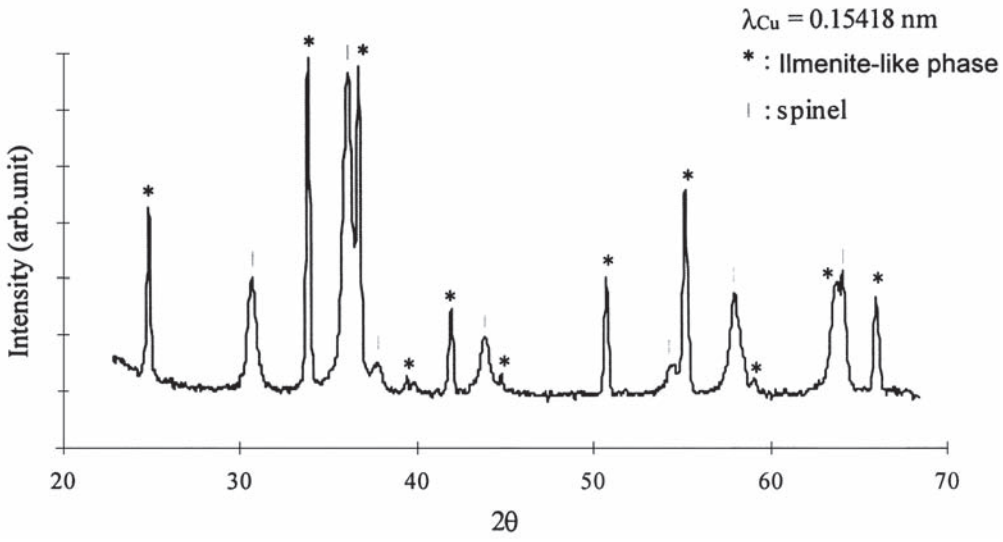

Fig. 6. X-ray pattern obtained after thermal treatment in air at 773 K for 100 h of $Ni_{0.70}Cu_{0.65}Mn_{1.65}\square_{3\delta/4}O_{4+\delta}$.

copper manganites synthesized at low temperature (623–673 K) are larger than 100 $m^2\ g^{-1}$, but for a fixed value of x_{Ni} the substitution of the manganese by copper leads to a decrease of Sw, whereas nickel has the opposite effect (Table 3). On the other hand, for a given oxide composition the specific surface area drops drastically with increasing the decomposition temperature of the oxalate (Table 4).

Upon heating such manganites synthesized at low temperature (623–673 K) in an inert atmosphere (argon) oxygen loss occurs, but X-ray diffraction shows that the spinel structure is conserved at least until 900 K. The example of $Ni_{0.28}Cu_{0.80}Mn_{1.92}O_4$ is given in Fig. 7. Moreover, the lattice parameters obtained at the end of the Temperature Programmed Reduction in argon are similar to those of the stoichiometric oxides (with the same chemical composition). These observations show that such oxides were initially non-stoichiometric and have lost their non-stoichiometry during the TPR.

Table 3
Evolution of the specific surface area Sw of $Ni_xCu_yMn_{(3-x-y)}\square_{3\delta/4}O_{4+\delta}$ (synthesized in air at 623 K) with their chemical composition

x_{Ni}	y_{Cu}	Sw ($m^2\ g^{-1}$)
0.30	0	165
0.30	0.33	155
0.70	0	190
0.70	0.26	180
0.70	0.65	160
0.70	0.75	155
0.70	0.91	140

Table 4
Evolution of the specific surface area Sw of $Ni_{0.70}Cuo_{0.65}Mn_{1.65}\square_{3\delta/4}O_{4+\delta}$ synthesized in air at different temperatures

T decomposition (K)	Sw ($m^2\ g^{-1}$)
623	160
673	120
693	96
723	64
773	32
873	11
973	7

The non-stoichiometry of these oxides can be explained by the presence of cations with larger oxidation states than in stoichiometric oxides [19], implying the presence of cationic vacancies. For instance, the presence of Ni^{3+} cations in spinel compounds has already been reported by several authors [20–22] in the cases of nickel and nickel–copper–manganites and nickel–zinc ferrites. The occurrence of trivalent nickel can be explained by the oxidation of some of the Ni^{2+} cations during the synthesis of the oxide in air at low temperature. In a similar manner, cations like Mn^{2+} and Mn^{3+} could

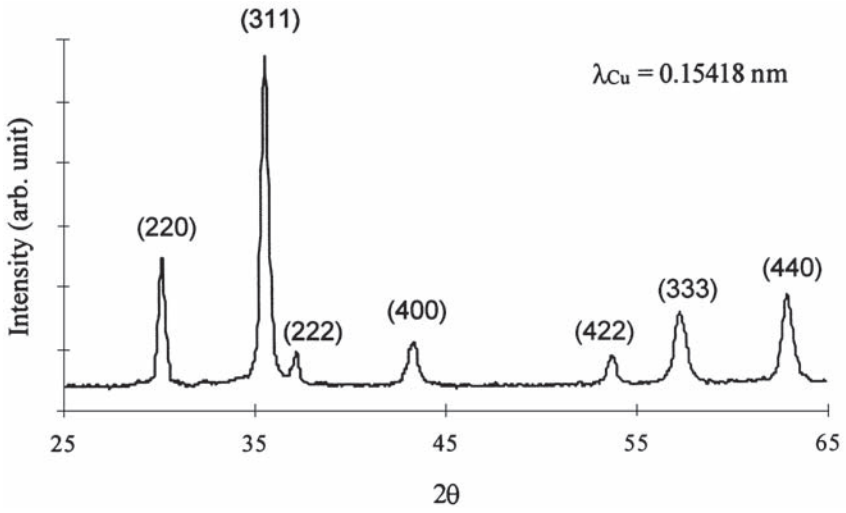

Fig. 7. XRD pattern of $Ni_{0.28}Cu_{0.80}Mn_{1.92}O_4$ after TPR in argon at 5 K min^{-1} up to 900 K.

also have undergone oxidations during the synthesis, leading, respectively, to Mn^{3+} and Mn^{4+}.

As illustrated in Table 5, δ depends on the decomposition temperature of the oxalate precursor (decreasing with increasing synthesis temperature) and is thus closely related to the specific area Sw of the oxide.

In order to follow and understand the evolution of δ with the chemical composition of the oxides, we considered first the cases of manganese oxide and nickel manganites synthesized by the same preparation route.

The manganese oxide obtained by thermal decomposition of manganese oxalate at 623 K in air for 6 h is the compound Mn_5O_8 as shown by its X-ray diagram compared to the JCPDS data (ref. 75-1427, see Fig. 8). Oswald et al. [23] who have determined the structure of Mn_5O_8 have shown that this oxide is isostructural with $Cd_2Mn_3O_8$, that is $Mn_2^{II}Mn_3^{IV}O_8$, in which the cations Mn^{2+} are in an uncommon six-fold coordination with six oxygens forming a distorted trigonal prism. These two oxides are monoclinic and crystallize in the C2/m space group.

Table 5
Evolution of Sw and δ for $Ni_{0.28}Cu_{0.80}Mn_{1.92}\square_{3\delta/4}O_{4+\delta}$ synthesized in air at different temperatures

T decomposition (K)	Sw (m^2 g^{-1})	δ
673	135	0.36
698	65	0.30
743	45	0.15
973	3	0

TPR experiments show that the Mn_5O_8 prepared at 623 K from thermal decomposition of manganese oxalate actually possesses a low non-stoichiometry and should thus be written $Mn_5O_{8+\delta}$ ($\delta = 0.06$) which can be explained by the oxidation of some Mn^{2+} cations to either Mn^{3+} or Mn^{4+} (Mn^{2+} being in a six-fold coordination in which both Mn^{3+} and Mn^{4+} can accommodate). This non-stoichiometry, creating local distortions in the crystal because of the substitution of some Mn^{2+} cations by Mn^{3+} or Mn^{4+} and involving cationic vacancies, may explain the differences between the lattice parameters (see Fig. 8) of the $Mn_5O_{8+\delta}$ prepared in this study at 623 K and those of the stoichiometric Mn_5O_8 determined by Oswald. On the contrary, the parameters of Mn_5O_8 heated in argon up to 720 K are very close to those of the stoichiometric oxide (Fig. 8).

In the case of nickel manganites, which exhibit the spinel structure, the results concerning their non-stoichiometry (see Table 6) show the impact of the nickel content on δ. Indeed, one can see clearly that δ reaches a maximum for ca. $x_{Ni} = 0.7$. Consequently, the introduction of nickel into the Mn–O system not only enables the transformation from the structure of Mn_5O_8 to the spinel, but also plays an important role in the number of cationic vacancies (determined by the non-stoichiometry), and therefore in the cationic

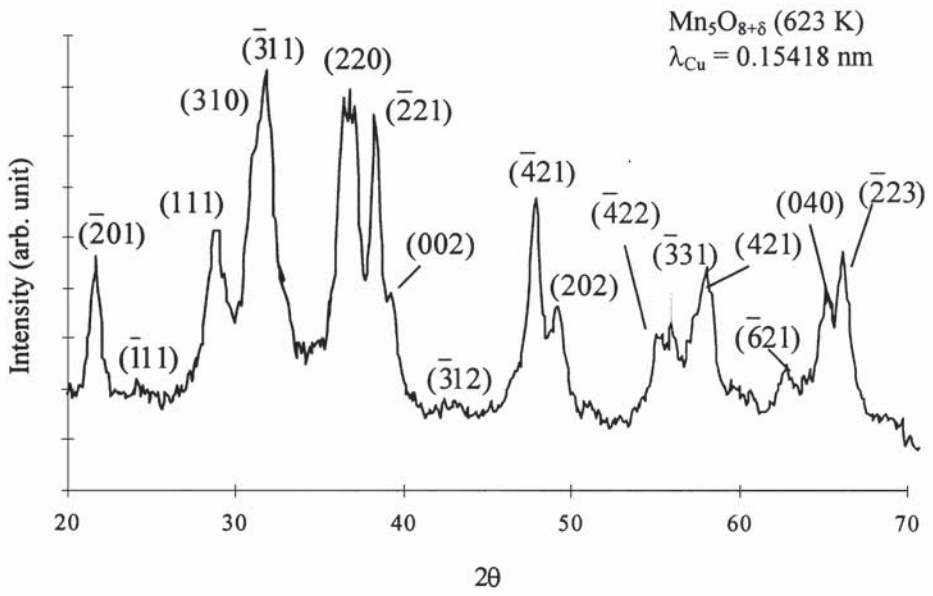

Experimental interplanar spacings (in Å) for $Mn_5O_{8+\delta}$ (623 K) and JCPDS data

(hkl)[1]	d (JCPDS)[1]	d (623 K)	(hkl)[1]	d (JCPDS)[1]	d (623 K)	(hkl)[1]	d (JCPDS)[1]	d (623 K)
(201)	4.0829	4.1031	(312)	2.1001	2.1070	(222)	1.5519	1.5532
(111)	3.6788	3.6833	(421)	1.8955	1.8963	(003)	1.5254	1.5226
(111)	3.1060	3.0875	(202)	1.8488	1.8480	(621)	1.4767	1.4773
(311)	2.7937	2.8130	(022)	1.7871	1.7866	(040)	1.4310	1.4285
(220)	2.4686	2.4372	(422)	1.6619	1.6610	(223)	1.4078	1.4106
(221)	2.3435	2.3443	(331)	1.6389	1.6389			
(002)	2.2881	2.2904	(421)	1.5863	1.5876			

[1] : data from JCPDS (ref. 72-1427)

Oxide	Lattice parameters (distances in Å)			
	a	b	c	β°
$Mn_5O_{8+\delta}$ (623 K)	10.441	5.638	4.838	109.10
Mn_5O_8 (TPR argon - 720 K)	10.394	5.722	4.845	109.37
Mn_5O_8 (JCPDS)[1]	10.347	5.724	4.852	109.41

[1] : data from JCPDS (ref. 72-1427)

Fig. 8. Experimental XRD pattern of $Mn_5O_{8+\delta}$ synthesized in air at 623 K, lattice parameters of $Mn_5O_{8+\delta}$ (623 K), Mn_5O_8 after TPR in argon at 720 K and JCPDS data.

distribution of the oxides. As stated above, the non-stoichiometry of nickel manganites could be explained by the existence of Ni^{3+} cations and/or the occurrence of supernumerary Mn^{3+} and Mn^{4+} ions.

The non-stoichiometry of nickel–copper manganites was determined from similar TPR experiments. Some of the results obtained are also given in Table 6. It can be pointed out that for oxides containing the same nickel amount, δ tends to decrease when the copper content of the oxide increases. However, as we showed before the introduction of copper leads to a decrease of the specific surface area of the oxide, which is closely related to δ. Hence, the decrease of the non-stoichiometry observed when the copper content increases could be partly due to this decrease of Sw. Attempts to prepare oxides with the same

Table 6
Non-stoichiometry δ of nickel and nickel–copper manganites $Ni_xCu_yMn_{3-x-y}\square_{3\delta/4}O_{4+\delta}$ synthesized in air at 623 K

	x_{Ni}	y_{Cu}	δ
(1)	0.30	0	0.48
(2)	0.45	0	0.51
(3)	0.70	0	0.66
(4)	0.80	0	0.60
(5)	1.05	0	0.43
(6)	0.30	0.33	0.47
(7)	0.30	0.80	0.37
(8)	0.70	0.26	0.51
(9)	0.70	0.65	0.27

composition and specific area but different δ (or vice versa) are in progress.

The typical reduction profiles obtained during the Temperature Programmed Reductions in argon of Mn_5O_8, a nickel manganite and a nickel–copper manganite have been reported in Fig. 9. These profiles can be divided into several successive steps whose intensity and position depend on the chemical composition of the initial oxide. These steps might be related to changes of oxidation states of some cations or to the appearance of more or less stable intermediates.

Such TPR data may bring information about the cationic distributions of these oxides. Navrotsky and Kleppa determined the octahedral or tetrahedral site preference energies for various divalent and trivalent cations in the spinel structure [24], showing in particular the preference of Ni^{2+}, Cu^{2+} and Mn^{3+} cations for octahedral sites and that of Mn^{2+} cations for tetrahedral sites. The oxidation states of the cations and the cationic distributions of stoichiometric nickel–copper manganites and copper manganites have been studied by many authors [2,25–32] but a great controversy remains concerning the proportions of copper ions in tetrahedral and octahedral sites and their ionic states. However, most of the authors agree with the presence of Cu^{+} cations in tetrahedral sites and Cu^{2+} in both octahedral and tetrahedral sites. Furthermore, Ni^{2+} cations may also be present in the two kinds of sites, at least for high nickel contents [33]. Non-stoichiometric nickel–copper manganites contain cations with higher oxidation states than in stoichiometric oxides and thus may present cationic distributions even more complex than those of stoichiometric oxides. At this time, our results do not enable us to propose reliable distributions but additional studies are in progress like electrical conductivity and surface analyses techniques such as XPS.

4. Conclusion

Nickel–copper–manganese mixed oxalates $Ni_{x/3}Cu_{y/3}Mn_{(3-x-y)/3}C_2O_4$, nH_2O were precipitated in aqueous solution at room temperature and characterized by thermal analyses and X-ray diffraction. A minimum nickel content of $x_{Ni}=0.1$ was necessary to synthesize Ni–Cu–Mn oxalates with mixed crystal structure, and for a given nickel amount $x_{Ni}\leq 0.1$, the oxalate precipitated was mixed up to a maximum limit of copper content (depending on x_{Ni}). Beyond this limit, copper oxalate was formed. The introduction of nickel made it possible to prepare mixed oxalates probably due to the intermediate crystalline structure of nickel oxalate (β) between those of manganese oxalate (α) and copper oxalate. Furthermore, X-ray diffraction showed that the structure (α or β) of the ternary oxalates obtained depended on their chemical composition, and particularly on their manganese content, the β form being predominant when the Mn amount was too low.

Nickel–copper manganites $Ni_xCu_yMn_{3-x-y}\square_{3\delta/4}O_{4+\delta}$ were synthesized by thermal decomposition of mixed Ni–Cu–Mn oxalates at low temperature (623–673 K). XRD experiments showed a stabilizing effect of copper for the spinel structure, which is an interesting feature when compared to nickel manganites. These oxides are highly divided since their specific surface areas Sw are in the range 100–200 $m^2\,g^{-1}$, but the introduction of copper tends to decrease Sw while nickel has an opposite effect. These oxides were found to be non-stoichiometric with cationic vacancies. Their non-stoichiometry δ was determined from chromatographic titration of the oxygen released during Temperature Programmed Reductions in argon. These experiments showed that δ depended both on the decomposition temperature of the oxalate and on the chemical composition of the oxide (δ decreasing with increasing copper amount). Such a non-stoichiometry can

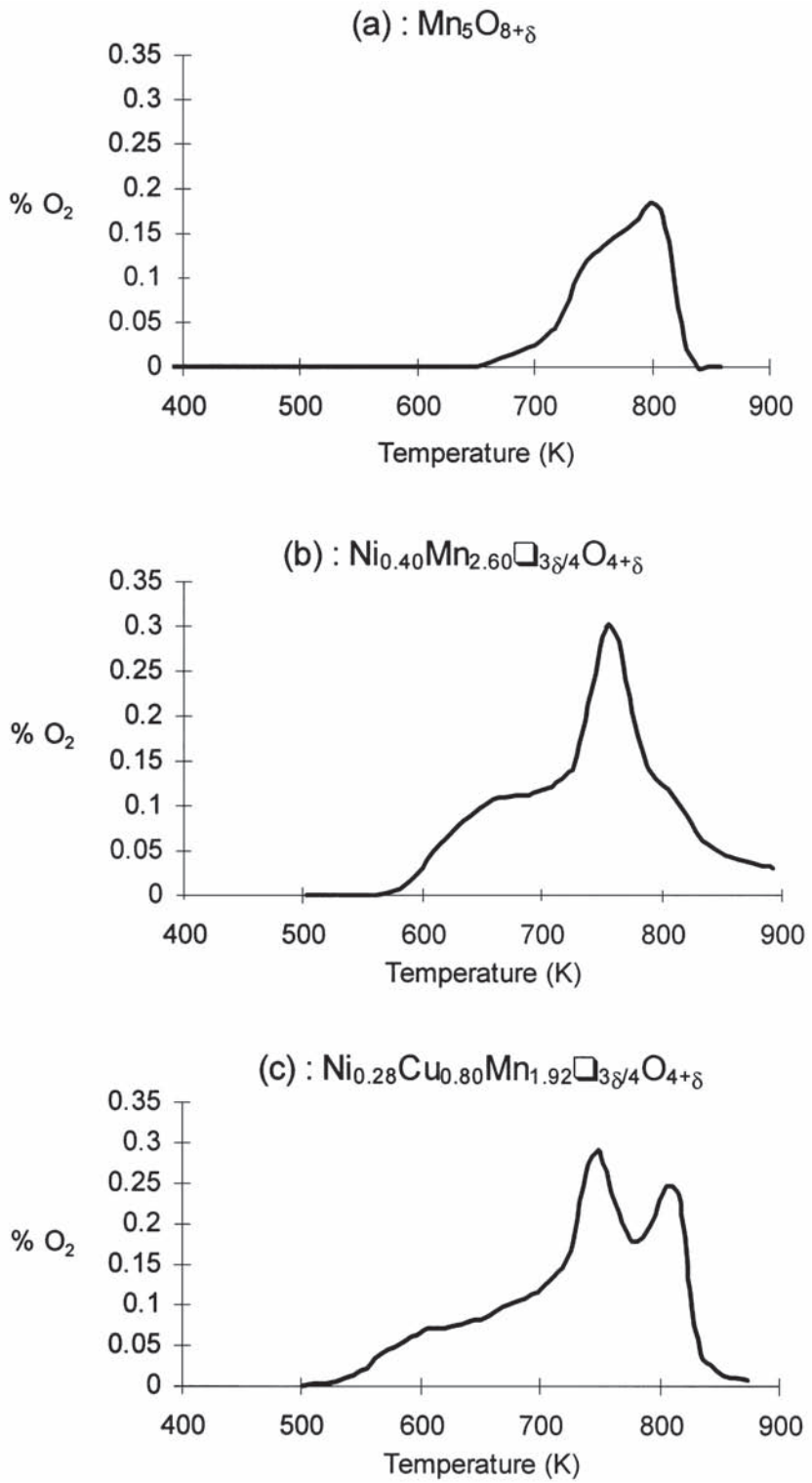

Fig. 9. Oxygen loss during TPR in argon of $Mn_5O_{8+\delta}$, $Ni_{0.40}Mn_{2.60}\square_{3\delta/4}O_{4+\delta}$ and $Ni_{0.28}Cu_{0.80}Mn_{1.92}\square_{3\delta/4}O_{4+\delta}$ synthesized in air at 623 K.

be explained by the presence of supernumerary cations such as Ni^{3+}, Cu^{2+}, Mn^{4+} and Mn^{3+} formed during the synthesis of the oxide at low temperature. These results may bring interesting information concerning the cationic distributions of such non-stoichiometric nickel–copper manganites.

References

[1] R. Metz, R. Legros, A. Rousset, J.P. Caffin, A. Loubière, Ai Bui, Silicates Ind. 3–4 (1990) 71.
[2] J.P. Caffin, A. Rousset, R. Carnet, A. Lagrange, in: P. Vincenzini (Ed.), Proc. World Congress of High Tech Ceramics, Amsterdam, 1987, p. 1743.
[3] W.H. Rhodes, J. Am. Ceram. Soc. 64–1 (1981) 19.
[4] S. Inada, T. Kimura, T. Yamagushi, Ceramics International 16 (1990) 369.
[5] C. Laberty, P. Alphonse, A. Rousset, MRS Symposium Proc. 497 (1998).
[6] J. Robin, Bull. Soc. Chim. Fr. (1953) 1078.
[7] H. Pezerat, J. Dubernat, J.P. Lagier, C. R. Acad. Sc. 266C (1968) 1357.
[8] F. Mazzi, C. Garavelli, Periodico di mineralogia 26 (1957) 269.
[9] R. Deyrieux, C. Berro, A. Péneloux, Bull. Soc. Chim. Fr. 1 (1973) 25.
[10] J.P. Lagier, H. Pezerat, J. Dubernat, Revue Chim. Min. 6 (1969) 1081.
[11] H. Fichtner-Schmittler, Cryst. Res. Tech. 19–9 (1984) 1225.
[12] A. Michalowicz, A. Girerd, J.J. Goulon, J. Inorg. Chem. 18 (1979) 3004.
[13] Handbook of Chemistry and Physics, CRC Press, 64th ed. (1983–1984) B91.
[14] C. Villette, P. Tailhades, A. Rousset, J. Sol. Stat. Chem. 117 (1995) 64.
[15] J. Töpfer, J. Jung, Thermochimica Acta 202 (1992) 281.
[16] D. Dollimore, Thermochimica Acta 117 (1987) 331.
[17] D.G. Wickham, J. Inorg. Nucl.Chem. 26 (1964) 1369.
[18] J. Töpfer, A. Feltz, Solid State Ionics 59 (1993) 249.
[19] X.X. Tang, A. Manthiram, J.B. Goodenough, J. Less Common Metals 156 (1989) 357.
[20] T. Hashemi, A.W. Brinkman, J. Mater. Res. 7–5 (1992) 1278.
[21] T. Hashemi, Br. Ceram. Trans. J. 90 (1991) 171.
[22] K. Majima, M. Hasegawa, M. Yokota, S. Mishima, H. Nagai, Mat. Trans. 34–6 (1993) 556.
[23] H.R. Oswald, M.J. Wampetich, Helv. Chim. Acta 50–7 (1967) 2023.
[24] A. Navrostky, O.J. Kleppa, J. Inorg. Nucl. Chem. 29 (1967) 2701.
[25] E. Elbadraoui, J.L. Baudour, F. Bouree, B. Gillot, S. Fritsch, A. Rousset, Solid State Ionics 93 (1997) 219.
[26] S. Veprek, D.L. Cocke, S. Kehl, H.R. Oswald, J. Catal. 100 (1986) 250.
[27] M. Lenglet, A. D'Huysser, J. Kasperek, J.P. Bonnelle, J. Durr, Mat. Res. Bull. 20 (1985) 745.
[28] V.A.M. Brabers, R.E. Vandenberghe, Phys. Lett. 44A (7) (1973) 493.
[29] J. Töpfer, A. Feltz, D. Graf, B. Hackl, L. Raupach, P. Weissbrodt, Phys. Stat. Sol. 134 (1992) 405.
[30] G.Y. Bandage, H.V. Keer, J. Phys. C: Solid St. Phys. 9 (1976) 1325.
[31] R.E. Vandenberghe, Phys. Stat. Sol. 50 (1978) K85.
[32] A.D.D. Broemme, V.A.M. Brabers, Solid State Ionics 16 (1985) 171.
[33] C. Laberty, M. Verelst, P. Lecante, P. Alphonse, A. Mosset, A. Rousset, J. Sol. Stat. Chem. 129 (1997) 271.